Journal of Power Sources 196 (2011) 2558–2566

Contents lists available at ScienceDirect

Journal of Power Sources

journal homepage: www.elsevier.com/locate/jpowsour

Reactant recirculation system utilizing pressure swing for proton exchange membrane fuel cell

Masatoshi Uno*, Takanobu Shimada, Koji Tanaka

Institute of Space and Astronautical Science, Japan Aerospace Exploration Agency, 3-1-1 Yoshinodai, Sagamihara, Kanagawa 252-5210, Japan

ARTICLE INFO

Article history:
Received 30 August 2010
Received in revised form 23 October 2010
Accepted 28 October 2010
Available online 4 November 2010

Keywords:
Fuel cell
Recirculation
Flow-through mode
Dead-end mode
Suction pressure

ABSTRACT

To minimize the wastage of supplied reactant, fuel cells need to be operated in either dead-end or recirculation modes. A fuel cell operating in a dead-end mode is not durable without periodic purging because of flooding; therefore, a little reactant is unavoidably wasted. Conventional recirculation systems employ mechanical pumps or ejectors as their recirculation devices, but they have drawbacks originating from the inherent properties of pumps and ejectors. This paper proposes a pumpless reactant recirculation system, the pressure swing recirculation system, which utilizes pressure swings produced by the reactant supply and consumption. This system requires only two check valves and a fluid control device, and operates by alternating between the equivalent flow-through and dead-end modes. The proposed system was applied for both anode and cathode of a PEMFC. A single cell was operated in dead-end and pressure swing recirculation modes for comparative analyses. The resultant cell performances in the dead-end mode deteriorated rapidly because of flooding, while those in the pressure swing recirculation using high-purity reactants were stable and durable over 10 h. The experimental results demonstrated that the pressure swing operation could expel the product water from the cell, and operations over 10 h were achievable as long as the purity of the supplied reactants was high enough.

1. Introduction

Fuel cell technologies, such as proton exchange membrane fuel cells (PEMFCs), direct methanol fuel cells, and solid oxide fuel cells, have been attracting attention as concerns about global warming and demands for high-energy power sources have increased. In particular, PEMFCs have been extensively studied and are still under intensive research and development, especially for automotive and stationary applications. PEMFCs are considered to be one of the most promising and viable power sources, useful not only for terrestrial applications but also for aerospace applications [1–3], including super-pressure balloons and moon explorations, which require small and light power systems at moderate operating temperature.

In general, reactants, such as hydrogen and oxygen, need to be excessively supplied to PEMFCs operating at low temperatures to prevent reactant starvation and to remove product water, which might lead to flooding that hinders the reactants from reaching the reaction sites inside the cell. Unreacted reactants and product water are discharged from the fuel cell outlet. However, discharging them into the ambient atmosphere reduces the reactant utilization of the fuel cell system. Unreacted hydrogen in the stationary applications can be burned and the produced heat is utilized for fuel reformers [4]. In applications without reformers, on the other hand, dead-end or recirculation systems are employed to minimize the reactant wastage.

Dead-end operations are those in which the outlet of the fuel cell is sealed to achieve high reactant utilization, and such systems are often employed [5–12]. Fuel cell systems for dead-end mode operations are very simple because of the absence of recirculation devices such as pumps and ejectors. However, the product water is prone to accumulate in the cell because of a lack of forced convection in the dead-end mode, which eventually causes the flooding and deterioration of the cell performance in the form of voltage decline. In general, water is produced in the cathode; however, even in the anode, water films and droplets can be found because of vapor condensation and back-diffused product water from the cathode. Therefore, periodic purging [5,6] or continuous purging [7,8] with a small flow rate is necessary to refresh or maintain the cell performance. During purging, the unreacted reactants are unavoidably discharged with the product water into the ambient atmosphere. In addition, purging causes the cell voltage in the dead-end mode to vary significantly, because the purging process starts when a predefined low voltage level is detected, and it is completed when either a certain period of time has elapsed or the cell has recovered a certain voltage level.

* Corresponding author. Tel.: +81 42 759 8366; fax: +81 42 759 8366.
E-mail address: uno.masatoshi@jaxa.jp (M. Uno).

0378-7753/$ – see front matter © 2010 Elsevier B.V. All rights reserved.
doi:10.1016/j.jpowsour.2010.10.094

The fuel cell systems for large energy applications employ a reactant recirculation system in which the unreacted reactants discharged from the outlet of the fuel cells are recirculated back to the inlet to minimize the reactant wastage [2,3]. The recirculation systems achieve a stable and durable operation without periodic purging processes, because continuous forced flow produced by the recirculation device can prevent water buildup in the cell. Conventional recirculation systems use mechanical pumps that consume electrical power and generate vibration and noise. In addition, the pumps consist of several mechanical components that are not desirable in terms of reliability and simplicity. Since the major advantages of fuel cells over conventional combustion generators include high efficiency, tranquility, and lack of vibration, the need to use mechanical pumps qualitatively neutralizes such benefits. Furthermore, the technical difficulty of hermetically sealing the fuel cell system can arise, because the pumps consist of special sealing parts such as bearings, diaphragms, and lubricants, all of which provide opportunities especially for hydrogen, the smallest molecule, to escape.

Ejectors can recirculate the unreacted reactants without using moving parts, and they have been studied for fuel cell recirculation systems [13–21]. They are advantageous over mechanical pump-based recirculation systems in terms of mechanical reliability and efficiency, and hence, they are considered promising. However, they are still under research and sophisticated computed fluid dynamics (CFD) analyses are necessary to design ejectors. Moreover, the ejectors operate almost passively and their performance is strongly influenced by their geometry and working conditions; hence, additional moving parts might be required to realize a wide operating range [18]. In the case of operations without the additional moving parts, the ejectors may work unstably during startup, shut-down, and load changes because their performance is inconstant in a low flow rate region, i.e., a low current density region for fuel cells. The flow characteristic in the low flow rate region tends to become complicated and unexpected fluctuations in the recirculation line could occur [19,20]. In addition, the influence of water existence in the unreacted reactant on the ejector performance is also a concern [21].

In this paper, we propose a pumpless reactant recirculation system, the pressure swing recirculation system, which utilizes pressure increase and decrease produced by reactant supplies and consumptions. Instead of recirculation devices, only two check valves and a fluid control device are required for recirculation. The fundamental operating principles, major benefits, control strategies for recirculation, and influence of pressure swing on the cell performance in the proposed system are explained and discussed. The pressure swing recirculation systems were built separately for both the anode and the cathode of a PEMFC. The experimental stability performance tests for a single cell supplied with pure hydrogen and oxygen were performed in both dead-end and pressure swing recirculation modes.

2. Pressure swing recirculation systems

2.1. Pressure swing recirculation in pressure-controlled mode

A schematic diagram of the proposed pressure swing recirculation system is shown in Fig. 1. For simplicity, only the anode system without a humidifier is depicted. Only two check valves and a fluid control device are needed for recirculation. A pressure controller is employed as the fluid control device for the pressure-controlled pressure swing recirculation. The reactant pressure of the fuel cell inlet is measured and controlled by the pressure sensor and the pressure controller, respectively. In this configuration, the pressure is directly controlled by the pressure controller, while

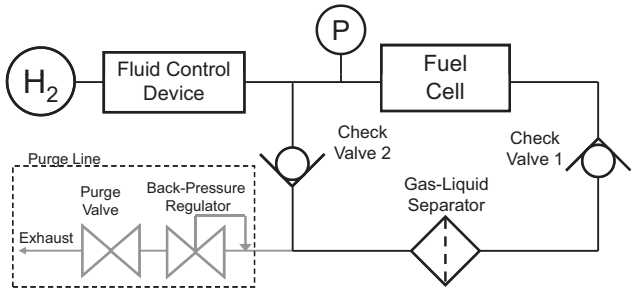

Fig. 1. Schematic diagram of pressure swing recirculation system.

the flow rate of the pressure controller is indirectly determined by the increase rate of the pressure, consumption rate of the reactant, and fluid volume of the piping. The pressure swing recirculation system operates in two modes, A and B, and these two modes alternate with each other. Reactant flow directions in each mode are depicted in Fig. 2(a) and (b), respectively. The theoretical operating waveforms are illustrated in Fig. 3. In the proposed system, the pressure varies between the predefined upper and lower limits, P_U and P_L, respectively.

In mode A, during the reactant supply period, the pressure controller increases the reactant pressure from P_L to P_U by introducing reactant into the fuel cell. The reactant supply rate must be greater than the reactant consumption rate in order to increase the pressure. The flow rate of the pressure controller, q_{in}, is expressed as

$$q_{in} = p_A C + q_{FC} = p_A(C_{\mathrm{Cont}} + C_{\mathrm{Check}}) + q_{FC} = p_A C_{\mathrm{Cont}} + q_{CV1} + q_{FC}, \quad (1)$$

where p_A is the pressure increase rate in mode A (i.e., the pressure increase per unit time), C is the total fluid volume, C_{Cont} is the fluid volume between the pressure controller and check valves (i.e., the volume of flow channels in the cell and the volume of piping directly connected to the cell), C_{Check} is the fluid volume of piping between check valves 1 and 2, q_{FC} is the reactant consumption rate, and q_{CV1} is the flow rate of the check valve 1.

As shown in Fig. 2(a), a part of the unreacted reactants passes through check valve 1 at a flow rate of q_{CV1}. Therefore, mode A

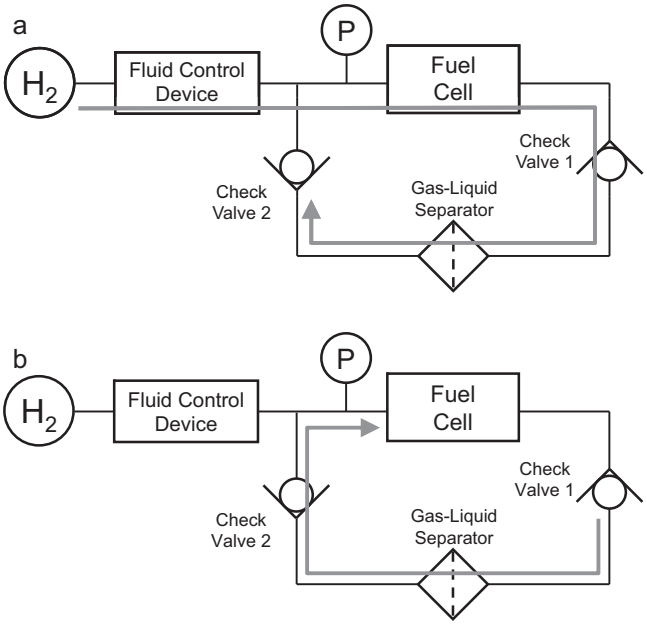

Fig. 2. Reactant flow directions in (a) mode A and (b) mode B.

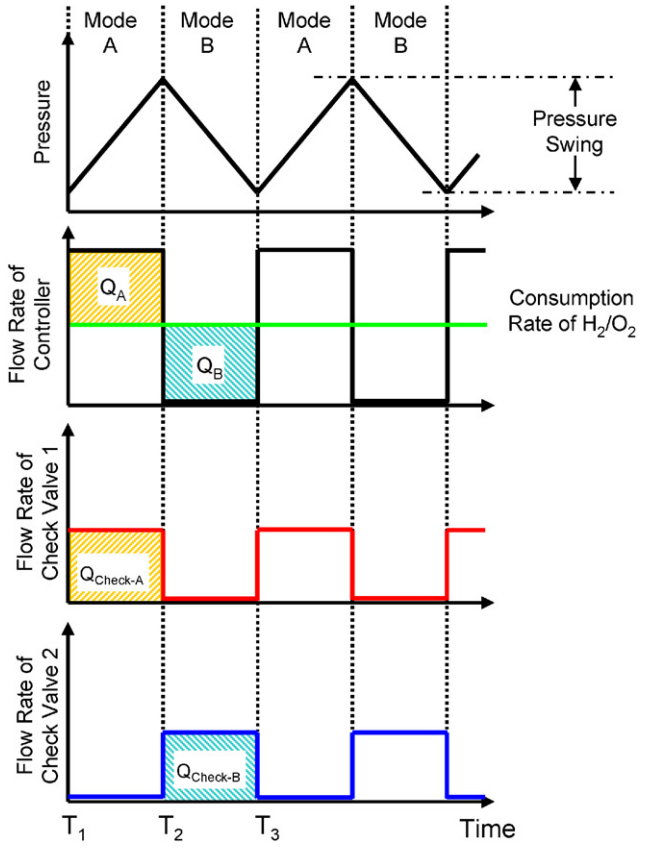

Fig. 3. Theoretical operating waveforms of pressure swing recirculation.

can be regarded as an equivalent flow-through mode, in which the unreacted reactant flows through check valve 1. Hence, the product water is removed from the cell by the reactant flow in this mode. Generally, in fuel cell stacks or multi-channel fuel cells, the larger flow rate is necessary to clear channels blocked with product water. By increasing p_A or q_{in}, the flow rate of the unreacted reactant becomes larger, and the blocked channels can be cleared.

The rest of the unreacted reactants accumulate in C_{Cont}, and their accumulation rate corresponds to $p_A C_{Cont}$ in Eq. (1). As long as p_A and q_{FC} are constants, q_{in} should also be constant. At that moment, the pressure on the primary side of check valve 2 is lower than that on the secondary side because of pressure losses in the fuel cell, check valve 1, and the piping. Therefore, check valve 2 is closed, and the part of the unreacted reactants whose flow rate corresponds to q_{CV1} accumulates in the piping between check valves 1 and 2. Mode A lasts until the reactant pressure reaches P_U. The amount of reactant accumulation, Q_A, which is indicated as the filled area in Fig. 3 is expressed as

$$Q_A = Q_{Cont\text{-}A} + Q_{Check\text{-}A} = \int_{T1}^{T2} (q_{in} - q_{FC})\,dt = C(P_U - P_L) = (C_{Cont} + C_{Check})(P_U - P_L), \quad (2)$$

where $Q_{Cont\text{-}A}$ and $Q_{Check\text{-}A}$ are the amounts of reactant accumulation in the fluid volume of C_{Cont} and C_{Check}, respectively, and are given by

$$\begin{cases} Q_{Cont\text{-}A} = \displaystyle\int_{T1}^{T2} (q_{in} - q_{FC} - q_{CV1})\,dt = C_{Cont}(P_U - P_L) \\ Q_{Check\text{-}A} = \displaystyle\int_{T1}^{T2} q_{CV1}\,dt = C_{Check}(P_U - P_L) \end{cases}. \quad (3)$$

$Q_{Check\text{-}A}$ is equal to the area indicated in Fig. 3.

In mode A, the reactant pressure in the piping between check valves 1 and 2, P_{Check}, is lower than that of the fuel cell, P_{FC}, due to the pressure loss in check valve 1, i.e., a cracking pressure. By assuming there is no pressure loss in the fuel cell, P_{Check} in mode A is given by

$$P_{Check} = P_{FC} - P_{Crack} \le P_U - P_{Crack}, \quad (4)$$

where P_{Crack} is the cracking pressure of the check valve.

After P_{FC} exceeds P_U, the pressure controller stops the reactant supply and shifts from mode A to mode B. The length of mode A, T_A, is

$$T_A = \frac{P_U - P_L}{p_A} = \frac{Q_A}{q_{in} - q_{FC}} = \frac{Q_{Cont\text{-}A}}{q_{in} - q_{FC} - q_{CV1}} = \frac{Q_{Check\text{-}A}}{q_{CV1}}. \quad (5)$$

Although there is no reactant supply from the controller, the fuel cell continues to consume reactants as long as it supplies electricity to the load. At the beginning of mode B, i.e., during the recirculation period, the residual reactants in C_{Cont} are consumed first (the flow directions of the residual reactants are not depicted in Fig. 2(b)). A suction pressure is simultaneously produced by the consumption of the residual reactants, and the pressure starts to decrease. At that point, the unreacted reactants that have accumulated in the piping between check valves 1 and 2 in mode A are drawn out through check valve 2 by the produced suction pressure, as illustrated in Fig. 2(b). As the accumulated reactants are consumed, the reactant pressure decreases. At that moment, check valve 1 is closed, because the pressure on the primary side of check valve 1 is lower than that on its secondary side because of pressure losses in the fuel cell, check valve 2, and the piping. The relationship between q_{FC} and the flow rate of check valve 2, q_{CV2}, in mode B is given by

$$q_{FC} = p_B C = p_B(C_{Cont} + C_{Check}) = p_B C_{Cont} + q_{CV2}, \quad (6)$$

where p_B is the pressure decrease rate in mode B (i.e., the pressure decrease per unit time). As long as q_{FC} is constant, the q_{CV2} should also be constant. In mode B, the reactant is supplied from C_{Cont} and C_{Check}, and there is no outlet flow, i.e., $q_{CV1} = 0$. Therefore, mode B can be regarded as an equivalent dead-end mode, in which the piping in the system behaves as a reactant supply source such as a reactant cylinder. In this mode, the product water is not actively removed because there is no forced flow in the cell.

The amount of reactant consumption in mode B, Q_B, which is indicated by the filled area in Fig. 3, is yielded as

$$Q_B = Q_{Cont\text{-}B} + Q_{Check\text{-}B} = \int_{T2}^{T3} q_{FC}\,dt = C(P_U - P_L) = (C_{Cont} + C_{Check})(P_U - P_L), \quad (7)$$

where $Q_{Cont\text{-}B}$ and $Q_{Check\text{-}B}$ are the amounts of reactant consumption in the fluid volume of C_{Cont} and C_{Check}, respectively, and are given by

$$\begin{cases} Q_{Cont\text{-}B} = \displaystyle\int_{T2}^{T3} (q_{FC} - q_{CV2})\,dt = C_{Cont}(P_U - P_L) \\ Q_{Check\text{-}B} = \displaystyle\int_{T2}^{T3} q_{CV2}\,dt = C_{Check}(P_U - P_L) \end{cases}. \quad (8)$$

In mode B, P_{FC} is lower than P_{Check} due to the cracking pressure of check valve 2. P_{Check} in mode B is given by

$$P_{Check} = P_{FC} + P_{Crack} \ge P_L + P_{Crack}. \quad (9)$$

From Eqs. (2) and (7), and Eqs. (3) and (8), Q_A and Q_B, $Q_{Cont\text{-}A}$ and $Q_{Cont\text{-}B}$, and $Q_{Check\text{-}A}$ and $Q_{Check\text{-}B}$ are determined to be equal in the steady-state condition, in which there is no change in q_{FC} every single cycle. The pressure decreases until it falls below P_L, and the pressure controller then begins reintroducing the reactants, and the

operation returns to mode A. The length of mode B is determined by

$$T_B = \frac{Q_B}{q_{FC}} = \frac{Q_{\text{Cont-}B}}{q_{FC} - q_{CV2}} = \frac{Q_{\text{Check-}B}}{q_{CV2}}. \quad (10)$$

From Eqs. (5) and (10), the cycle period, T_P, can be yielded as

$$T_P = T_A + T_B = Q\frac{q_{in}}{q_{FC}(q_{in} - q_{FC})}, \quad (11)$$

where $Q = Q_A = Q_B$.

From Eqs. (4) and (9), the pressure criterion for realizing the pressure swing recirculation is yielded as

$$P_U - P_L \geq 2P_{\text{Crack}}. \quad (12)$$

To secure the pressure swing recirculation, $P_U - P_L$ is desired to be large enough. However, as discussed in Sections 2.3 and 2.4, a moderate value of $P_U - P_L$ should be used to keep a cell voltage fluctuation low.

Alternation between modes A and B makes reactant recirculation feasible. The product water is expelled with the unreacted reactants from the fuel cell outlet in mode A, i.e., the equivalent flow-through mode, although it just accumulates inside the cell in mode B, i.e., the equivalent dead-end mode. The product water contained in the unreacted reactants is removed using the gas–liquid separator placed between check valves 1 and 2 to avoid flooding. However, similar to the conventional recirculation system, inactive substances contained in the supplied reactants cannot be removed by recirculation. Therefore, when a buildup of inactive substances grows and degrades the cell performance, the system must be purged to refresh the cell performance by releasing the purge valve shown in Fig. 1.

The reactant pressure in the proposed system varies inevitably; hence, the negative influence of mechanical stress, induced by the pressure swings, on the membranes is a concern. Tang et al. investigated the fatigue strength of the Nafion membrane [22]. They considered that the stress generated by gas, which is usually not more than 1 MPa, is not high enough to cause a serious damage to the membranes. Based on their study, the pressure swings are deduced not to be mechanically harmful to the membranes.

The proposed recirculation system, which actively utilizes suction pressure produced by reactant consumption for the recirculation, does not require any pumps, and offers several benefits. The major benefits of the proposed system over the conventional systems using mechanical pumps are as follows:

1. The proposed system achieves higher efficiency because the power consumption of fluid control devices, such as pressure controllers and flow controllers, are much lower than that of the mechanical pumps.
2. Good tranquility is realized because of the lack of mechanical pumps.
3. The proposed system is considered more mechanically reliable. Although some moving parts, such as check valves and fluid control devices, are required, the total number of moving parts can be reduced.
4. The proposed system consists of only ordinary piping parts; hence, the concerns about hermeticality can be mitigated dramatically.

The above benefits such as high efficiency, good tranquility, high mechanical reliability, and good hermeticality, are also true for ejector-based recirculation systems. However, as mentioned in Section 1, the existence of product water in the unreacted reactant and operations in the low flow rate region lead to unstable performance of ejectors. The proposed system, on the other hand, does not have limitations in terms of the operating range and existence of water, and thus is able to operate stably even in such conditions. Therefore, the proposed recirculation system is considered advantageous over the ejector-based system in terms of operating range and stability.

The proposed recirculation system offers a number of benefits over conventional systems using mechanical pumps or ejectors. However, a cell voltage in the proposed system inevitably fluctuates due to consecutive cycles of equivalent flow-through and dead-end modes. In the conventional systems, on the other hand, the cell voltage is stable because the unreacted reactant is recirculated continuously. An issue of the cell voltage fluctuation which is a disadvantage of the proposed system is discussed in Section 2.3.

2.2. Pressure swing recirculation in flow-controlled mode

The reactant pressure can be adjusted by a flow controller instead of the pressure controller. For the flow-controlled pressure swing recirculation, the flow controller is employed as the fluid control device in Fig. 1. The fundamental operating principles, such as the flow directions shown in Fig. 2, the operating waveforms shown in Fig. 3, and Eqs. (1)–(12), are identical to the operating principles of the pressure-controlled mode explained in the previous section. In this mode, however, the pressure increase rate, p_A, cannot be directly controlled because of the absence of the pressure controller. Instead of p_A, flow rate of the controller, q_{in}, is directly controlled by the flow controller.

To realize pressure swing recirculation, the reactant pressure must increase in mode A, or p_A must be greater than zero. Transforming Eq. (1) as follows yields

$$q_{in} - q_{FC} = p_A C = p_A(C_{\text{Cont}} + C_{\text{Check}}) > 0, \quad (13)$$

implying that q_{in} must be higher than q_{FC}. To keep q_{in} higher than q_{FC}, the generated current should be measured such that q_{in} can be actively controlled by a current-sensing feedback. By assuming $q_{in} = \lambda_A \times q_{FC}$ ($\lambda_A > 0$), Eq. (13) can be rewritten as

$$q_{FC}(\lambda_A - 1) = p_A C = p_A(C_{\text{Cont}} + C_{\text{Check}}) > 0, \quad (14)$$

where λ_A is the stoichiometric ratio in mode A.

From Eqs. (5), (10), and (14), the ratio of T_A to T_B can be determined as

$$T_A : T_B = 1 : \lambda_A - 1. \quad (15)$$

The recirculation system using the flow controller can determine the ratio of T_A to T_B by controlling λ_A without knowing the fluid volumes of the piping.

2.3. Cell voltage during pressure swing recirculation

In the proposed pressure swing recirculation system, the pressures of the reactants vary inevitably between P_U and P_L. Based on a Nernst equation, which expresses an electromotive force of a chemical cell, the cell voltage of the fuel cell is dependent on the partial pressures of the reactants; hence, the pressure swing causes inevitable fluctuations in the cell voltage. In addition, alternations between two different flow modes influence the cell voltage. In mode A, the reactants actively flow from upstream to downstream of the fuel cell, such that a concentration overvoltage (or concentration loss), which tends to be significant when the reactant supply rate is not high enough, is comparatively low. On the other hand, in mode B, in which the cell is operated equivalently in a dead-end mode as explained in the previous section, the concentration overvoltage tends to be high. Thus, from two viewpoints, the Nernst equation and concentration overvoltage, the lowest cell voltage can be found at the end of mode B. Furthermore, there is another factor that decreases the cell voltage in mode B, as explained in the next section.

With a constant current load, only the cell voltage fluctuates as explained above. With a constant voltage load, on the other hand, the pressure swing recirculation causes fluctuations in a cell current instead of voltage. In that case, any parameters dependent on q_{FC}, such as q_{in}, p_A, and T_P, are also influenced because q_{FC} is proportional to the cell current. Hence, a period of the pressure-induced cell voltage fluctuation is influenced. If the cell is operated at a constant power, both the cell voltage and current fluctuate.

2.4. Accumulation of inactive substances in the system

Although the supplied reactants were designated as "pure" hydrogen and oxygen, they usually contain impurities. In closed fuel cell systems, such as dead-end and recirculation systems, such impurities, i.e., inactive substances, eventually accumulate in the systems. The amount of inactive substances gradually grows and the concentrations of the reactants decrease as the cumulative amount of reactant consumption increases.

The amount of inactive substances in the systems, Q_X, is expressed as

$$Q_X = \int x q_{in}\, dt, \tag{16}$$

where x is the concentration of the inactive substances contained in the supplied reactants. In the closed fuel cell system, q_{in} is basically equal to q_{FC}; hence,

$$\int q_{in}\, dt = \int q_{FC}\, dt. \tag{17}$$

The concentration of the inactive substances in the system, X, can be expressed as

$$X = \frac{Q_X}{P_{FC}C} = \frac{x}{P_{FC}C} \int q_{FC}\, dt. \tag{18}$$

Since the voltage of a fuel cell is dependent on the partial pressures of reactants, as expressed by the Nernst equation, an increase in X leads to a decrease in the cell voltage. Furthermore, Eq. (18) implies that X varies even in a single cycle as P_{FC} swings. At the end of mode B, when P_{FC} is the lowest (i.e., P_L), X becomes the highest in a single cycle, and the cell voltage should be the lowest from the viewpoint of reactant concentration.

The cell voltage in the closed fuel cell system unavoidably decreases as the inactive substances accumulate in the system. If the cell voltage decreases severely due to this accumulation, the system needs to be purged to reduce X. The cell voltage performance can be refreshed by discharging inactive substances into the ambient atmosphere [6].

2.5. Influence of humidification on pressure swing recirculation

In the previous sections, the pressure swing system without a humidifier was discussed and a volume of water vapor was neglected. This section discusses the influence of humidification on the pressure swing recirculation.

After the reactant passes through the humidifier, which is not depicted in Fig. 1, the reactant contains water vapor to some extent depending on humidification temperature. And the piping between the fuel cell and humidifier is heated to prevent vapor condensation. Therefore, the reactant supply rate, q_{in}, with humidification is equivalently greater than that without humidification, although the substantial reactant flow rates are identical. Since the product water is discharged from the fuel cell outlet, the unreacted reactant also contains water vapor even in nonhumidified systems. However, in general, the piping after the fuel cell is not heated, so that the vapor pressure of the unreacted reactant is low enough to be negligible. In the humidified systems, therefore, only parameters dependent on q_{in} are influenced by the humidification.

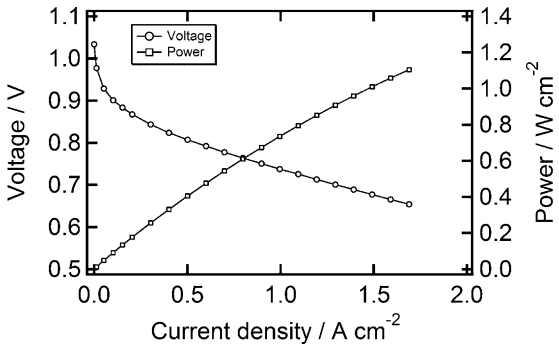

Fig. 4. Characteristics of the proton exchange membrane single fuel cell used in the experiments.

According to Eq. (5), the larger value of q_{in} makes p_A and T_A greater and shorter, respectively, in the flow-controlled mode. In the pressure-controlled mode, on the other hand, p_A is controlled by the pressure controller, and T_A is not influenced by the humidification because T_A is determined by p_A, not by q_{in}. In mode B, T_B is simply determined by q_{FC} as expressed by Eq. (10), and not influenced by the humidification. Thus, the period of the pressure swing in the flow-controlled mode is influenced by the humidification though the pressure swing recirculation works even with humidifiers.

3. Experimental

A single cell with an active area of 49 cm^2 was used in the experiments. The membrane electrode assembly (MEA) consisted of Nafion 112, Pt/C electrodes with a Pt catalyst loading of 1.0 mg cm^{-2} on both anode and cathode, and GDLs (Toray, TGP-H-060) with 30 wt% PTFE content. Single-serpentine flow channels with depths and widths of 1.0 mm each were used for both the anode and cathode flow fields. Fig. 4 shows the reference characteristic of the single cell operated at a nonhumidified pressurized condition of 200 kPa (abs.) with dry pure hydrogen and oxygen. The cell temperature was 75 °C, and the stoichiometries of hydrogen and oxygen were 2.0 each.

The recirculation systems were built for both the anode and the cathode without humidifiers. The experimental recirculation system was as same as shown in Fig. 6, though, in which only the anode system is depicted for simplicity (water drain and electrical systems are not depicted). Nonhumidified pure hydrogen (>99.99%, standard grade) and oxygen (>99.5%, standard grade, or >99.999%, G2 grade) were supplied to the cell. Anode and cathode recirculation tests were separately performed using a pressure controller (HORIBA STEC, UR-7340) or mass flow controllers (HORIBA STEC, SEC-E40). These controllers were connected in series, and the pressure controller was located downstream of the mass flow controller. In the pressure-controlled mode, the pressure and mass flow controllers were enabled and disabled, respectively, and in the flow-controlled mode, vice versa. Check valves with a cracking pressure of 7.1 kPa (Swagelok, CHS4) and a gas–liquid separator (Swagelok, SS-FCG) with a small fluid volume were used. To maintain the fluid volume of C_{Check} as constant as possible, an automatic water drain system was built using a combination of level sensors (OMRON, E2K-L13MC1) and an electromagnetic valve.

The cell was operated at 200 kPa (abs.) 75 °C in the flow-through mode until it reached the steady-state condition. After the steady-state condition was observed, the operation mode was switched to the dead-end mode or the pressure swing recirculation mode. In the anode recirculation experiments, the hydrogen pressure was

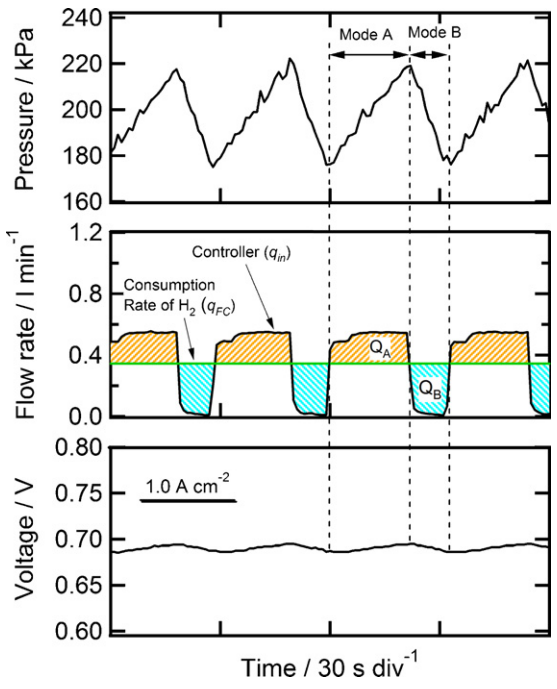

Fig. 5. Resultant waveforms of the fuel cell operated at 1.0 A cm^{-2} during pressure-controlled anode pressure swing recirculation.

swung while the cathode was kept in the flow-through mode, and for cathode recirculation, the process was vice versa. The purge valve was closed for the entire period of the recirculation tests except for the purging process. The reactant pressure for the flow-through mode was set using back-pressure regulators (Swagelok, KBP1E). The reactant pressures at the inlet of the fuel cell were measured using pressure sensors (KEYENCE, AP-13S) and were processed by an in-house LabVIEW software program to control the pressure controller and flow controller. P_U and P_L were 180 and 220 kPa (abs.), and 185 and 215 kPa (abs.) for anode and cathode recirculations, respectively. In the pressure-controlled mode operation, p_A was set to 2 kPa s^{-1}. In the flow-controlled mode operations, λ_A was 2.0. Stoichiometries for the flow-through mode were also 2.0.

4. Results and discussion

4.1. Operating waveforms in pressure-controlled anode pressure swing recirculation

The experimental waveforms of the anode inlet pressure, the flow rate of the pressure controller, and the cell voltage are shown in Fig. 5. The resultant waveforms are almost identical to the theoretical ones shown in Fig. 3. At the beginning of mode A, however, stair-step changes in the flow rate of the pressure controller, q_{in}, were observed, and it is considered to be due to the cracking pressure of the check valves. In general, to permit fluids to flow through a check valve, the pressure difference between the upstream and downstream sides of the check valve must be greater than the cracking pressure at which the check valve starts opening. Hence, at the beginning of mode A, check valve 1 was closed until the upstream pressure, i.e., the pressure at the fuel cell outlet, exceeded the cracking pressure. Therefore, at the beginning of mode A, the reactants accumulated only in the piping before check valve 1 and not in the piping between check valves 1 and 2. In other words, q_{CV1} was zero at the beginning of mode A. The values of q_{in} at the beginning and end of mode A were 0.49 and 0.55 l min^{-1}, respectively. Based on these values and q_{FC} of approximately 0.34 l min^{-1} at 1.0 A cm^{-2}, C_{Cont} and C_{Check} were determined to be approximately 1.25 and 0.50 ml kPa^{-1}, respectively, by Eq. (1). The amount of reactant accumulation and consumption in modes A and B, which are designated as filled areas of Q_A and Q_B in Fig. 5, were almost identical at approximately 70 ml. These obtained values were in good agreement with Eqs. (2) and (7).

The cell voltage fluctuated as the hydrogen pressure swung. However, the voltage fluctuations in the anode pressure swing recirculation were comparatively small and the overall performance was almost stable.

4.2. Operating waveforms in flow-controlled anode pressure swing recirculation

The resultant waveforms at current densities of 1.0 and 0.1 A cm^{-2} in the flow-controlled anode pressure swing recirculation mode are shown in Fig. 6(a) and (b). The length of modes A and B, T_A and T_B, were nearly equal because of λ_A = 2.0, as expressed by Eq. (15). As indicated by Eq. (11), the larger the current density which is proportional to q_{FC}, the shorter the period of the pressure swing was obtained. The values of Q_A and Q_B were calculated to be approximately 83 ml, and were independent on the current density because they are determined by P_U, P_L, and C, as expressed by Eqs. (2) and (7). The values of Q_A and Q_B in the flow-control mode were larger than those in the pressure-control mode. In the experimental system, the pressure controller was located downstream of the mass flow controller. Therefore, in the pressure-controlled mode, the fluid volumes of piping only after the pressure controller contributed to C_{Cont}. In the flow-controlled mode, however, not only the piping located after the pressure controller but also the piping between the flow controller and pressure controller were included in C_{Cont}. The total fluid volume was determined to be approximately 2.1 ml kPa^{-1} in the flow-controlled mode.

In the flow-controlled mode, because the supplied flow rate was controlled to a constant rate by the flow controller in mode A, there was no stair-step flow rate increase. However, the pressure in mode A was not as linear as in the pressure-controlled mode shown in Fig. 5. At the beginning of mode A, the reactants accumulated only in the piping before check valve 1, because check valve 1 was considered to be closed until the upstream pressure reached its cracking pressure. Therefore, based on Eq. (1), q_{CV1} was zero and the pressure increase rate, p_A, was comparatively steeper at the beginning of mode A. After the pressure exceeded the cracking pressure, p_A became gentler as q_{CV1} increased.

4.3. Stability performance in anode dead-end mode and pressure swing recirculation mode

The resultant stability performances at the current densities of 1.0 and 0.1 A cm^{-2} in the anode dead-end mode and in the flow-controlled pressure swing recirculation mode are shown in Fig. 7. In the operations at the current density of 1.0 A cm^{-2}, the cell voltage in the dead-end mode declined as the time elapsed and fell below 0.4 V, 1 h after the operation began, whereas the continuous operation over 10 h was achieved in the pressure swing recirculation mode. Although the cell voltage fluctuated as the pressure swung, it was stable for the entire periods. In the operations at the current density of 0.1 A cm^{-2}, on the other hand, the cell voltages were stable and durable in both modes. Thus, the effectiveness of the anode pressure swing recirculation at 0.1 A cm^{-2} was not verified.

If the steep voltage decline in the 1.0 A cm^{-2} dead-end mode was due to the buildup of inactive substances contained in the supplied hydrogen, the voltage at 1.0 A cm^{-2} in the pressure swing recirculation also had to decline steeply. Based on Eq. (18), the concentration of inactive substances at 200 kPa (abs.) in the anode 1 h

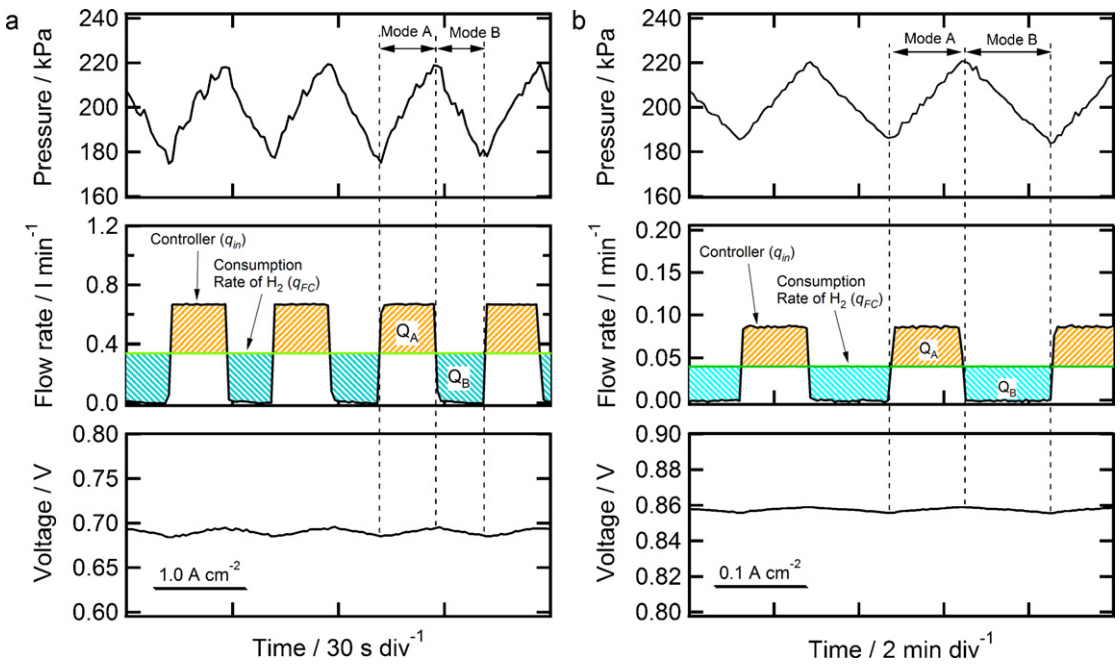

Fig. 6. Resultant waveforms of the fuel cell operated at (a) 1.0 A cm^{-2} and (b) 0.1 A cm^{-2} during flow-controlled anode pressure swing recirculation.

and 10 h after the operation at 1.0 A cm^{-2} began were determined to be approximately 0.47% and 4.7%, respectively, which were not high enough to deteriorate the cell performance. Therefore, we concluded that the voltage decline in the anode dead-end operation at 1.0 A cm^{-2} was due to flooding caused by the vapor condensation and/or by product water coming from the cathode in the form of back-diffusion, as reported in previous studies [5,9,11]. The stable performance at 0.1 A cm^{-2} was considered to be due to a small production rate of water. These experimental results indicated that the product water was effectively removed from the anode of the cell by the pressure swing recirculation.

4.4. Operating waveforms in flow-controlled cathode pressure swing recirculation

The resultant waveforms at a current density of 1.0 A cm^{-2} in the flow-controlled cathode pressure swing recirculation are shown in Fig. 8. The waveforms in the cathode pressure swing mode were similar to those in the anode recirculation, but the oxygen flow rate of the flow controller in mode B tapered gradually, whereas the hydrogen flow rate showed steep convergence to zero, as shown in Fig. 6. This phenomenon was presumably caused by a trait of the oxygen flow controller.

Based on the experimental data and Eq. (1), the total fluid volume of the cathode system was determined to be approximately 1.27 ml kPa^{-1}. The values of Q_A and Q_B were approximately 38.2 ml. The cell voltage fluctuations in the cathode recirculation were larger than those in the anode recirculation. In general, diffusivity of oxygen is much lower than that of hydrogen; hence, the concentration overvoltage in the cathode can be larger than that of

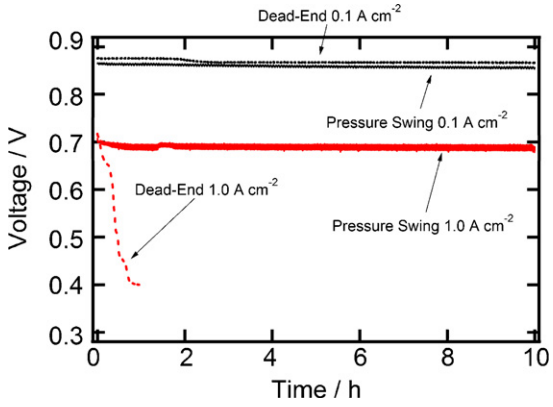

Fig. 7. Stability performances in anode dead-end mode and pressure swing recirculation.

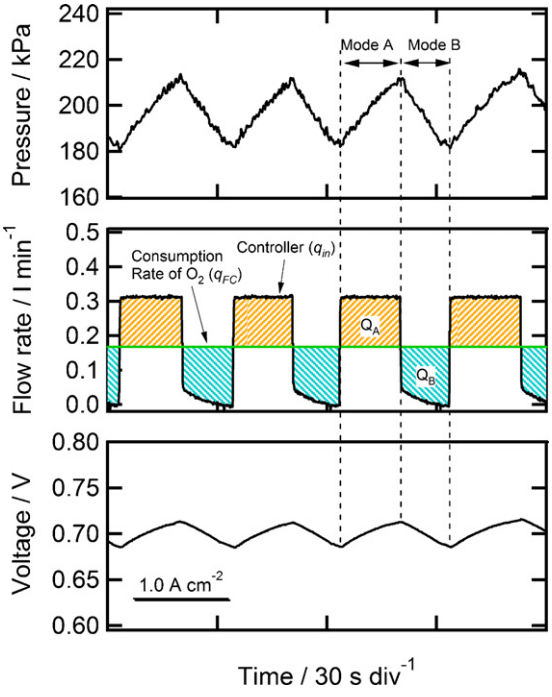

Fig. 8. Resultant waveforms of the fuel cell operated at 1.0 A cm^{-2} during flow-controlled cathode pressure swing recirculation mode.

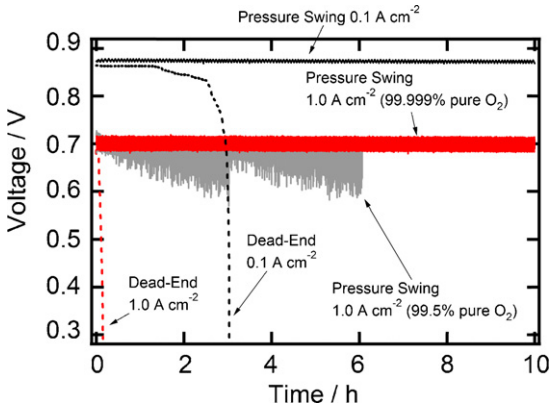

Fig. 9. Stability performances in cathode dead-end mode and pressure swing recirculation.

the anode under the same stoichiometric conditions. Therefore, the larger fluctuations in the cell voltage were considered to reflect the larger concentration overvoltage.

4.5. Stability performance in cathode dead-end mode and pressure swing recirculation

The experimental cell voltage trend at the current densities of 1.0 and 0.1 A cm^{-2} in the cathode dead-end mode and in the flow-controlled pressure swing recirculation mode are shown in Fig. 9. The cell voltage at 1.0 A cm^{-2} in the dead end mode decreased with time, consistent with that in the anode dead-end mode. However, the rate of the voltage decline was steeper. The cell voltage fell below 0.3 V within 8 min after the experiment began. Moreover, even the cell voltage at 0.1 A cm^{-2} declined though it took longer time to reach 0.3 V. Product water is produced on the cathode electrode and leads to flooding, which hinders the oxygen from reaching the reaction sites unless it is removed. There was no forced convection inside the cell operating in the dead-end mode; hence, the product water accumulated rapidly and caused severe flooding, which deteriorated the cell voltage. This result ascertained that the stable operation in cathode dead-end mode is infeasible and the cathode needs to be operated in either the flow-through mode or recirculation mode for long-term operations.

Continuous operation was achieved by the pressure swing recirculation using 99.5% pure oxygen, although the cell voltage fluctuated with swings in the pressure. The obtained continuous performance indicated that the product water was removed by the pressure swing recirculation. However, as time elapsed, the voltage fluctuation tended to increase and the cell voltage gradually decreased. The voltage finally reached approximately 0.6 V, 3 h after the operation began. At that moment, the cathode system was purged for 10 s by opening the purge valve. The purging process recovered the cell voltage to almost the initial voltage level, and the cell voltage then started decreasing gradually again. During the purging, the stoichiometric ratio controlled by the flow-controller was also 2.0.

Since the exhaustion flow rate during purging (i.e., q_{CV1}) was identical to that in mode A, the purging process was deduced not to cause dramatic water removal. Therefore, we inferred that the gradual decrease in the cell voltage was initiated by the buildup of inactive substances contained in the supplied oxygen, and the recovery in the cell voltage was due to the reduction in the concentration of inactive substances. By assuming that there was no permeation of the inactive substances between the anode and the cathode, and using Eq. (18), the concentrations of the inactive substances, X, was calculated to be approximately 56% and 65% at P_U and P_L, respectively, 3 h after the operation began. These obtained

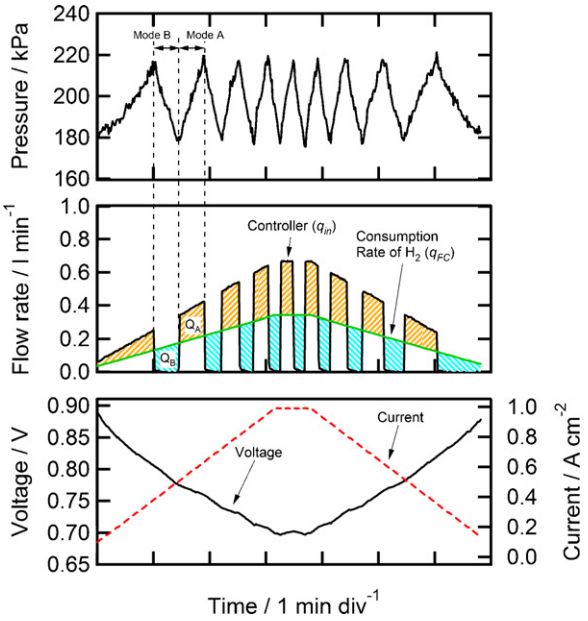

Fig. 10. Resultant dynamic performance of anode pressure swing recirculation during ramp change in load current.

values were high enough to degrade the cell performance.

In the pressure swing recirculation using 99.999% pure oxygen, the cell voltage at the current density of 1.0 A cm^{-2} was stable over 10 h and did not show a gradual decrease. The value of X at 200 kPa (abs.), 10 h after the experiment began, was determined to be 0.67% by Eq. (18), indicating that X had a negligible effect on the cell voltage. Therefore, by comparing the results shown in Fig. 9, we concluded that the gradual decrease in the cell voltage in the pressure swing recirculation using 99.5% pure oxygen was due to the accumulation of the inactive substances, not the buildup of the product water. These experimental results demonstrated that the pressure swing recirculation could remove the product water from the cell, and the 10 h operation was achievable as long as the purity of the supplied reactant was high enough.

The cell voltage at 0.1 A cm^{-2} in the pressure swing recirculation was also stable over 10 h. This result demonstrated that the pressure swing recirculation could work successfully even in the low current density region for the fuel cell, i.e., the low flow rate region in which the ejector performance is inconstant and may become unstable as mentioned in Section 1.

4.6. Dynamic performance of pressure swing recirculation during load changes

In most applications, the load power, and thus the current is not constant. Dynamic performances of the flow-controlled pressure swing recirculation were also investigated with ramp and step changes in the load current, i.e., the current density of the cell, for examples.

The dynamic performance during the ramp change is shown in Fig. 10. The current density of the cell was ramped up and down at the rate of 0.3 A cm^{-2} min^{-1} between 0.1 and 1.0 A cm^{-2}. In the flow-controlled mode, the cell current is monitored to control the flow rate of the controller, q_{in}, with the current-sensing feedback as mentioned in Section 2.2. q_{in} during mode A is always controlled to be λ_A times larger than the consumption rate of H_2, q_{FC}, as indicated by Eqs. (13) and (14), and the period of the pressure swing, T_P, which is determined by Eqs. (5), (10), and (11), is dependent on q_{FC}. Therefore, q_{in} and T_P gradually changed as the current density changed. Since the pressure increase and decrease rates, p_A and p_B,

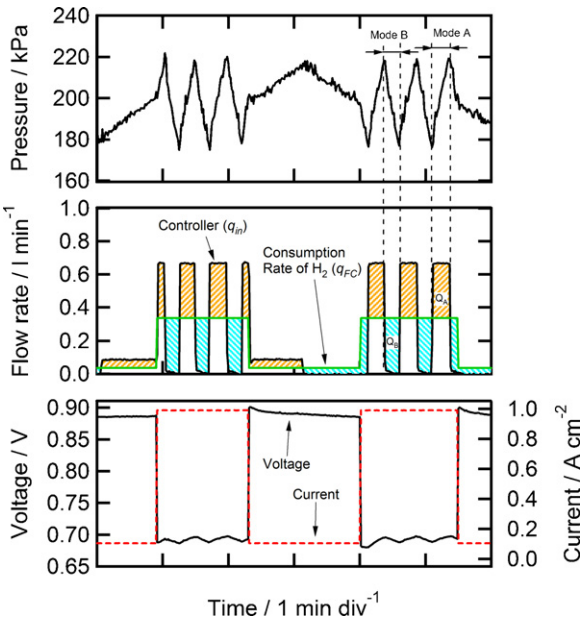

Fig. 11. Resultant dynamic performance of anode pressure swing recirculation during step change in load current.

in modes A and B, are dependent on q_{FC}, as expressed by Eqs. (14) and (6), respectively, they also changed gradually.

The dynamic performance during the step change is shown in Fig. 11. The current density of the cell was changed between 0.1 and 1.0 A cm^{-2}. As soon as the current change was detected, q_{in} and T_P immediately changed. Although p_A and p_B also changed immediately, there was no step change in the pressure because the change in the load current or q_{FC} only affects p_A and p_B.

The pressure swing recirculation worked well even during both ramp and step changes in the load current. In this paper, only the dynamic performances in the flow-controlled pressure swing recirculation were shown as the examples. However, as long as the fluid control device operates appropriately to control the reactant supply rate or the pressure increase rate, the pressure swing recirculation works even during such load changes.

5. Conclusions

We proposed a novel pumpless reactant recirculation system, the pressure swing recirculation system, which utilizes suction pressure produced by reactant consumption. The fuel cell in the proposed system operates by alternating between equivalent flow-through and dead-end modes. The pressure swing recirculation system requires only two check valves and a fluid-control device, and is advantageous over the conventional systems using mechanical pumps in terms of efficiency, tranquility, the ability to hermetically seal the system, and reliability. And it is able to operate stably under existence of product water even in a low flow rate region in which the performance of ejector-based system becomes unstable. The fundamental operating principle and the control strategies using a pressure controller or flow controller were discussed.

Experimental pressure swing recirculation operations were carried out for both the anode and the cathode. The resultant operating waveforms were almost identical to the theoretical ones, and the cell voltage fluctuations synchronizing with the pressure swings were observed. The voltage fluctuations in the cathode pressure swing were greater than those in the anode pressure swing. The lower diffusivity of oxygen was inferred to produce larger concentration overvoltage, and resulted in larger voltage fluctuations.

Experimental stability performance tests in the dead-end mode or pressure swing recirculation were performed for both the anode and the cathode. The cell performance in the anode pressure swing recirculation was stable over 10 h, whereas the anode dead-end mode operation led to a decline in the cell voltage within 1 h. Cathode dead-end operation was almost infeasible because of severe flooding, while the pressure swing recirculation achieved continuous operation. The cathode pressure swing operation using 99.5% pure oxygen showed a gradual decrease in the cell voltage and the voltage fluctuation tended to increase, while that using 99.999% pure oxygen demonstrated that the cell voltage was stable and durable over 10 h. The experimental results indicate that the pressure swing recirculation can remove the product water from the cell and stable operations over 10 h are achievable as long as the purity of the supplied reactant is high enough.

The dynamic performances of the pressure swing recirculation during ramp and step changes in the load current were also evaluated. As long as the fluid control device operates appropriately, the pressure swing recirculation worked well even during such load changes.

References

[1] M. Uno, T. Shimada, Y. Ariyama, N. Fukuzawa, D. Noguchi, K. Ogawa, H. Naito, Y. Sone, Y. Saito, J. Power Source 193 (2009) 788–796.
[2] Y. Sone, M. Ueno, S. Kuwajima, J. Power Source 137 (2004) 269–276.
[3] Y. Sone, M. Ueno, H. Naito, S. Kuwajima, J. Power Source 157 (2006) 886–892.
[4] J. Larminie, A. Dicks, Fuel Cell Systems Explained, second ed., Wiley, Chichester, England, 2003, pp. 252–263.
[5] J.W. Choi, Y.S. Hwang, J.H. Seo, D.H. Lee, S.W. Cha, M.S. Kim, J. Hydrogen Energy 35 (2010) 3698–3711.
[6] N. Bussayajarn, H. Ming, K.K. Hoong, W.Y.M. Stephen, C.S. Hwa, J. Hydrogen Energy 34 (2009) 7761–7767.
[7] W.H. Zhu, R.U. Payne, B.J. Tatarchuk, J. Power Source 156 (2006) 512–519.
[8] R.K. Ahluwalia, X. Wang, J. Power Source 171 (2007) 63–71.
[9] Ph. Moçotéguy, F. Druart, Y. Bultel, S. Besse, A. Rakotondrainibe, J. Power Source 167 (2007) 349–357.
[10] O. Himanen, T. Hottinen, S. Tuurala, Electrochem. Commun. 9 (2007) 891–894.
[11] T. Yang, P. Shi, J. Hydrogen Energy 33 (2008) 2795–2801.
[12] Y. Lee, B. Kim, Y. Kim, J. Hydrogen Energy 34 (2009) 7768–7779.
[13] A.Y. Karnik, J. Sun, J.H. Buckland, Am. Control Conf. Minneapolis (2006) 484–489.
[14] F. Marsano, L. Magistri, A.F. Massardo, J. Power Source 129 (2004) 216–228.
[15] M.L. Ferrari, A. Traverso, L. Magistri, A.F. Massardo, J. Power Source 149 (2005) 22–32.
[16] A. Vasquez, 6th International Energy Conversion Engineering Conference (IECEC) in Cleveland, AIAA, 2008, pp. 2008–5741.
[17] J.H. Lee, A. Sameen, V.R.S. Kumar, H.D. Kim, 41st AIAA/ASME/SAE/ASEE Joint Propulsion Conference and Exhibit in Tucson, AIAA, 2005, pp. 2005–3590.
[18] J.H. Lee, V.R.S. Kumar, H.D. Kim, 42nd AIAA/ASME/SAE/ASEE Joint Propulsion Conference and Exhibit in Sacramento, AIAA, 2006, pp. 2006–4884.
[19] Y. Zhu, Y. Li, J. Power Source 191 (2009) 510–519.
[20] Y. Zhu, W. Cai, Y. Li, C. Wen, J. Power Source 185 (2008) 1122–1130.
[21] M. Kim, Y.J. Shon, C.W. Cho, W.Y. Lee, C.S. Kim, J. Power Source 176 (2008) 529–533.
[22] H. Tang, S. Peikang, S.P. Jiang, F. Wang, M. Pan, J. Power Source 170 (2007) 85–92.